

# Segmentation and three-dimensional visualisation of digital in-line holographic microscopy data

Karen M. Molony

Department of Computer Science

National University of Ireland Maynooth

Maynooth, Co. Kildare, Ireland

[kmolony@cs.nuim.ie](mailto:kmolony@cs.nuim.ie)

Thomas J. Naughton

Department of Computer Science

National University of Ireland Maynooth

Maynooth, Co. Kildare, Ireland

and

University of Oulu

RFMedia Laboratory

Oulu Southern Institute, Vierimaantie 5, 84100 Ylivieska, Finland

[tomn@cs.nuim.ie](mailto:tomn@cs.nuim.ie)

## Abstract

*This paper demonstrates that transmissive or partially transmissive scenes imaged by digital in-line holographic microscopy (DIHM) can be reconstructed as a three-dimensional (3-D) model of the imaged volume from a single capture. This process entails numerical reconstruction, segmentation and polygonisation. Numerical reconstruction of a digital hologram captured using a DIHM set up is performed at equally spaced depths within a range. In the case of intensity modulating objects, segmentation of each of the reconstructed intensity images produces a contour slice of the scene by applying an adaptive threshold and border following. These slices are visualised in 3-D by polygonising the data using the marching cubes algorithm. We present experimental results for a real world DIHM capture of a partially transmissive scene that demonstrates the steps in this process.*

**Keywords:** Digital in-line holographic microscopy, segmentation, three-dimensional visualisation

## 1. Introduction

Holography [1, 2] is an imaging science made up of two parts, recording and replay. Traditionally, photographic films were used to record holograms. A hologram encodes 3-D information; intensity and directional information of the optical wave-front. Digital holography is derived from conventional holography but uses a digital area sensor instead of a photographic medium in order to capture the holograms, and reconstruction is performed on a computer numerically [3, 4]. This has only recently become feasible due to advances in computer technology and CCD sensors with high spatial resolution and high dynamic range. The microscopic principle originally proposed by Gabor [1] is the simplest realization of holography and has been coined digital in-line holographic microscopy (DIHM) [5]. It is this optical recording set up that we use in this paper.

Typical microscopy approaches, e.g. confocal microscopy, require dyes to make (quasi-)transparent biological samples, which are compressed between glass slides, visible. DIHM enables biological specimens to be analyzed at a cellular level in a completely unaltered environment in 3-D. Manual analysis of this data by a biologist is a tedious process. A further difficulty is introduced when using DIHM data as DIHM is an emerging technology with which biologists are not yet familiar. This is compounded by the

fact that the DIHM data is 3-D data. Extraction of 3-D data from DIHM data and subsequent analysis is an unsolved problem.

In this paper we focus on visualising 3-D features of scenes imaged by DIHM. In order to achieve this, reconstructions at various depths are obtained. A two part segmentation process is applied. An adaptive thresholding step, and then a border following step comprises the two-dimensional (2-D) segmentation that is applied to each of these reconstructions. The marching cubes algorithm is then implemented on the multiple segmented images to polygonise the dataset. This renders the surface of the volume that was imaged and so a 3-D segmentation and visualisation technique for DIHM is presented.

In section (2) an overview of the DIHM set up and reconstruction process is described. Further explanation of this type of optical setup can be found in [6]. The segmentation approach used is detailed in section (3). In section (4) a description of the marching cubes algorithm is provided. We present some experimental results in section (5) and we conclude in section (6).

## 2. Digital In-Line Holographic Microscopy

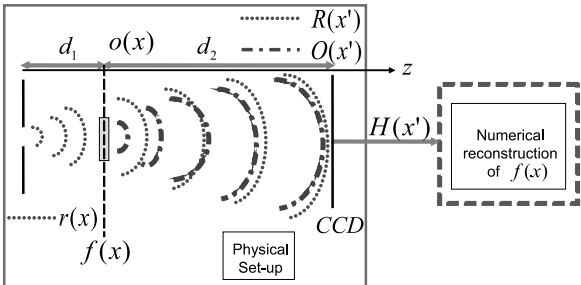


**Figure 1. DIHM set up is physically comprised of a light source, pinhole, sample, CCD and a computer for numerical processing.**

The first of the two stages of holography involves the recording of an interference pattern from an object beam and a reference beam. The second stage is replaying the wavefront of the original object from this recording. The output of the numerical reconstruction is typically a 2-D description of the wavefront at a single distance from the camera. The DIHM set up requires only a point light source, a pinhole, a transmissive or partially transmissive scene to be imaged, and an intensity recording device. This is suitable for biological samples [5] which are (quasi-)transmissive.

As shown in Fig.1, a spherical diverging beam  $r(x)$  emerges from a pinhole illuminating an object,  $f(x)$ , a distance  $d_1$

away. Immediately behind this plane there is an object wave,  $o(x) = f(x)r(x)$ . The interference pattern,  $H(x')$ , between the propagated reference wave,  $R(x')$ , and the propagated object wave,  $O(x')$ , is captured on a CCD a further distance  $d_2$  away. This capture is the input to the numerical reconstruction part of the imaging system.

Reconstruction of a capture obtained by this set up is possible on a computer by numerically calculating a diffraction integral that describes the diffraction in free space by the recorded hologram [7]. The sampling conditions for the Fresnel integral have been formalised [8, 9] and numerical approximations of the Fresnel transform (FST) have been applied successfully for digital hologram reconstruction [9, 10, 11]. Some fast algorithms for calculating free space Fresnel diffraction patterns have been developed [12, 13] and are applied for reconstructing the DIHM holograms in the experiments described.

## 3. Segmentation

In image processing, segmentation subdivides an image into regions. In digital holography, not all parts of a 3-D imaged object will necessarily be in-focus in a given 2-D reconstruction at a specific depth. Segmentation can be performed on a single reconstruction at a specific depth, or on multiple independently focused reconstructions at different depths [14], which, when combined can be considered a topography of the scene. In conventional digital holography a range of perspectives allow manipulation of the scene to overcome occlusions [15]. In DIHM such a range is not available due to the proximity of the components in the set-up. However, as DIHM is applied to transparent objects, retrieving segmentations at multiple depths can be achieved without the obstruction of occluding features. At any given depth, a reconstruction will show features in-focus at that depth and all out-of-focus features with reduced clarity [14]. Applying an adaptive threshold to filter out-of-focus features in an intensity reconstruction of a DIHM capture allows a successful application of border following.

### 3.1. Adaptive Threshold

In order to remove out-of-focus background features from a reconstructed intensity image a threshold can be applied. It is assumed that the in-focus features are brighter with respect to the background than out-of-focus features. A straightforward threshold is not as applicable if the background is not even. There is ample opportunity for noise to enhance an uneven background in a DIHM reconstruction, for example the DC term and twin image [16], speckle noise

[17], and out-of-focus features themselves can influence the background. Therefore an adaptive threshold [18] is applicable. An example of adaptive thresholding is shown in Fig.2. OpenCV [19] provides an implementation of this

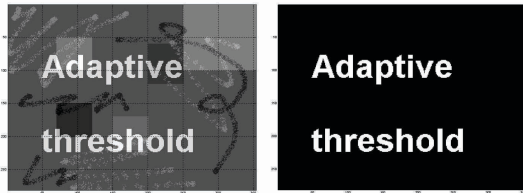


**Figure 2. Adaptive thresholding applied to the text on the left with an inconsistent background produces the binary result on the right hand side.**

which we apply in the grayscale region  $\{0-255\}$  on block sizes  $\approx 2\%$  of our image using mean weighting of pixels. The variable threshold is the weighted average of pixels within a block minus an offset. This provides a binary image of foreground and background features.

### 3.2. Border following

Border following is an algorithm that takes a binary image as input and outputs the borders of the objects and holes within those objects in the image. By indexing into the 2D raster, each pixel is checked to see if it is a foreground pixel. Once such a boundary pixel is found, i.e. the previous pixel was a background pixel, its connected pixels are examined. Usually the next pixel to be checked is in the same direction that has just been found. This process is repeated for each subsequent connected neighbour pixel, tracing the boundary until no more connected border pixels are found. Typically boundaries of the object are assumed to be in 8-connectivity and boundaries of holes to be in 4-connectivity [20] and so can be treated distinctly in the output. An example of border following is shown in Fig.3.

OpenCV provides an implementation of this based on [20]. The output is a contour, or a list of points that comprise a curve in an image [19]. This list can be manipulated to only consider contours in a given range of lengths, using a-priori knowledge of sought features to limit the number of false feature boundaries isolated.

## 4. 3-D visualisation

As segmentation is applied at a range of depths, a stack of binary contour images can be obtained and a volume



**Figure 3. Border following applied to the binary input on the left with a size restrucution results in the image on the right.**

is constructed from these. The data is now represented by slice segmentations through the scene. There are various scanning technologies that obtain data which is stored in a similar manner, e.g. confocal microscopy and magnetic resonanace imaging (MRI). The significant difference with DIHM data is that the slices are all obtained from a single capture and the volume is not physically scanned. Therefore movement of a sample is not a consideration. Furthermore no alteration of the sample is required, e.g. in confocal microscopy fluroescence or chemical dyes are required. Some 3D visualisation techniques of data stored in this way been explored [21]. Marching cubes [22] is an algorithm that was developed specifically for visualising this type of data and has proved effective for the polygonisation of similar scalar data [23].

### 4.1. Marching Cubes

Marching cubes [22] is an algorithm that generates triangles to represent surfaces. A 3D raster is subdivided into cubes. Each vertex of the cube is numbered 0–7 as shown in Fig.4.

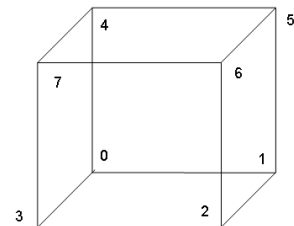


**Figure 4. A volume is subdivided into cubes. The vertices of such a cube are numbered 0–7**

Based on the values of the vertices of the cube with respect to an isosurface value, that cube is considered to be wholly inside or outside of a surface, or intersected by a surface. If some vertices are higher than the isosurface value and some are lower then trangles are drawn on the edges of the cube to

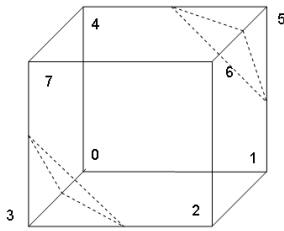


**Figure 5. Triangles drawn for a cube where only vertex 3 and vertex 5 are below the iso-surface**

demonstrate the intersections. There are  $2^8$  possibilities and so a known look up table is used which returns a twelve bit result, one for each edge of the cube, to show intersections on this cube. A look up table of corresponding triangles is also provided for computational efficiency. An example is shown in Fig.5 where vertex 3 and 5 are below the isosurface and the resulting intersecting triangles are drawn.

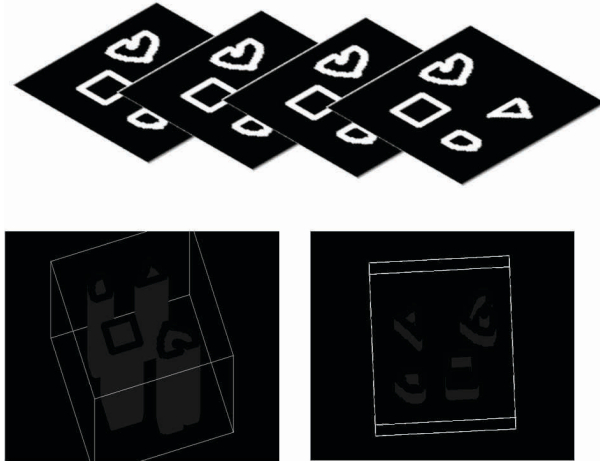


**Figure 6. For a stack of a repeated contour image, above, a 3-D rendering can be constructed of the surfaces and viewed from different perspectives, below.**

An example of marching cubes applied to a stack of the same input binary image is shown from two different perspectives in Fig.6.

## 5. Experimental Results

In this paper we detail the steps involved in the segmentation and visualisation of transmissive or partially transmissive scenes. These steps are illustrated here using a hologram of a cross hair sample captured using a DIHM set up.

While this is not ideal as hair is opaque, this hologram does allow for the demonstration of the process as the opaque sample is small with respect to the imaged scene.

A digital hologram of two hairs at one depth from the camera, and a single hair at a different depth were imaged by the DIHM process described previously as shown in Fig. 7. The scene can be reconstructed numerically from this sin-

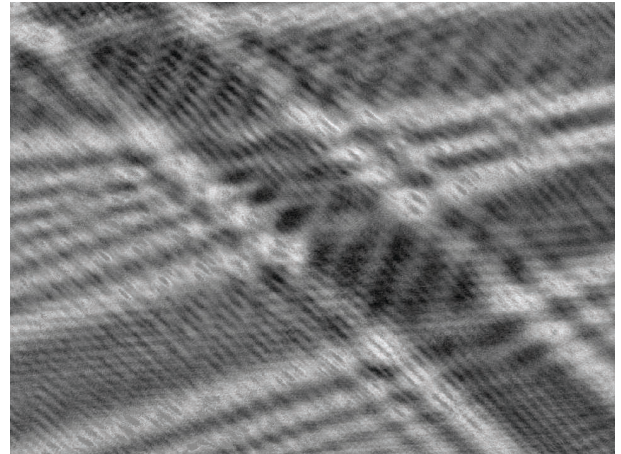


**Figure 7. Hair hologram captured using a DIHM set up**

gle capture so that the foreground cross hairs and the single background hair can be displayed in focus separately. In Fig. 8.A and 8.B numerical reconstructions of the scene are presented at a reconstruction depth of 235 mm and 300 mm respectively. Note that the reconstruction distances are the physical distances magnified. A human hair is  $\approx 100 \mu\text{m}$  thick. Reconstructions for depths ranging from {200–335} mm in steps of 5 mm were computed. the results of applying an adaptive threshold to the images shown in Fig.8 are shown in Fig.9. Following on from this, border following was applied for each thresholded result and the resulting contours were saved individually for further processing where each result represents a contour slice through the scene at that reconstruction depth. Examples of con-

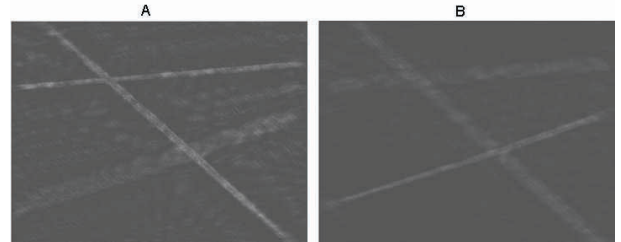


**Figure 8. A. Reconstruction at depth = 235 mm, B. reconstruction at depth = 300 mm**

mm in steps of 5 mm were computed. the results of applying an adaptive threshold to the images shown in Fig.8 are shown in Fig.9. Following on from this, border following was applied for each thresholded result and the resulting contours were saved individually for further processing where each result represents a contour slice through the scene at that reconstruction depth. Examples of con-

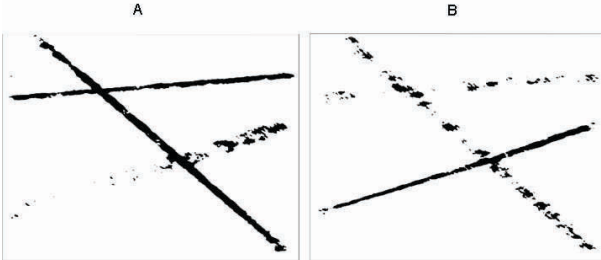


**Figure 9. A,B are thresholds of Fig.8.A,B**

tour slices corresponding to the reconstructions shown in Fig.8 are shown in Fig.10. Since we only consider contours  $\geq 1000$  pixels, noise arising from out-of-focus features is omitted from the contour slice.

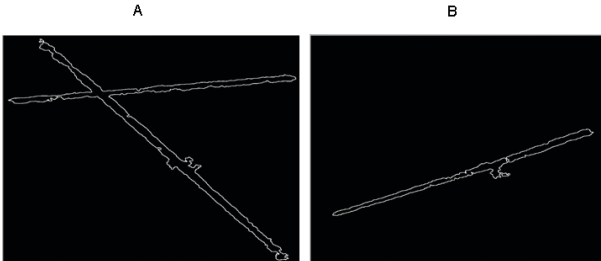


**Figure 10. A,B are contours of Fig.9.A,B**

The previously computed stack of contour slices comprises the 3-D input raster for the marching cubes algorithm. As the experimental sample is non-transmissive, contours are of the hairs in-focus and nearly in-focus, and so a 3-D type representation can be made. However, for a transmissive sample contour slices are of in-focus features only through the scene so a 3-D model representative of the volume can be obtained. As can be seen in Fig.11 the polygonsied surface of the scene can be viewed from any angle. The cross hairs at one plane, intersecting on the left hand side in both views in Fig.11, can be seen at a different depth than the single hair by looking at the z-axis shown.

As mentioned, the contour slices here are for the in-focus and nearly in-focus hairs and so the 3-D representation is not showing a 3-D model of the hair but rather the outline of those in the x-y plane at a range of depths. It is expected that a 3-D visualisation of a transmissive biological sample would appear more like the test example shown in Fig. 12 where each contour slice represents the exact boundaries of in focus features at that depth. The test sample is constructed from a stack of the same 2-D segmentation of a hologram of a 2-D sample of mammalian cells on a glass slide which is shown in the top left corner.

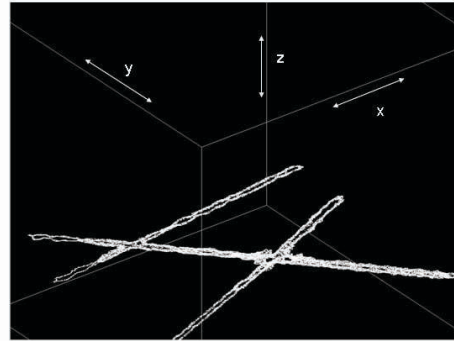
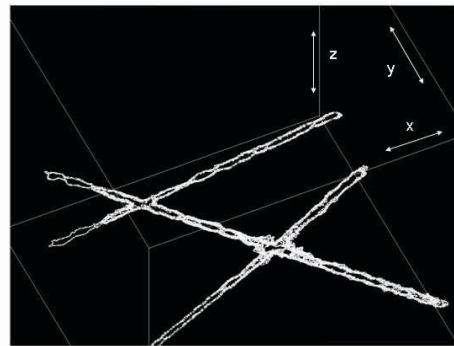


**Figure 11. Two different perspectives of a 3-D visualisation of contour slices**

## 6. Conclusions

We have shown that multiple 2-D segmentations of a scene at different depths can be obtained from a single hologram of a transmissive or partially transmissive scene. These 2-D segmentations can be used to then model a 3-D surface of the imaged sample. This is achieved by first applying an adaptive threshold to numerical reconstructions for a range of depths of a single digital hologram captured using a DIHM set up. Then border following is applied to the resulting binary image which produces a list of contours. Only contours within a specified range of lengths are selected. These lists are segmented slices, or contour slices, of the in-focus features at the corresponding reconstruction depth. Finally these contour slices are input to the marching cubes algorithm in order to polygonise the surface. This allows a 3-D visualisation of the imaged sample. The steps involved in this process were demonstrated using a test case of a real world hologram of hair. Future work on this topic requires DIHM captures of volumes of transmissive samples.

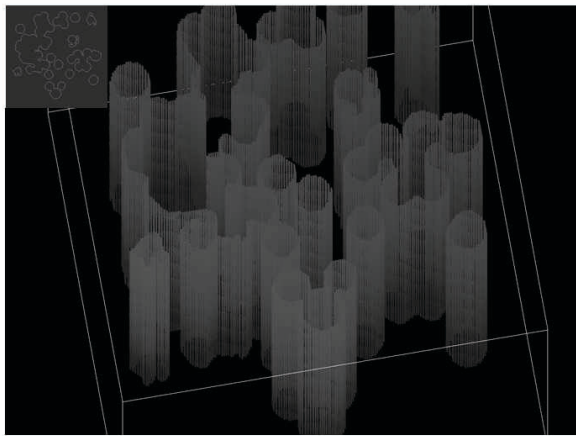


**Figure 12. 3-D visualisation of 200 repeated 2-D contour slices, shown at the top left corner, of a transmissive sample**

## References

- [1] D. Gabor, “A new microscopic principle,” *Nature*, vol. 161, pp. 777–778, 1948.
- [2] E. N. Leith and J. Upatnieks, “Wavefront reconstruction with diffused illumination and three-dimensional objects,” *J. Opt. Soc. Am.*, vol. 54, pp. 1295–1301, 1964.
- [3] T. M. Kreis, *Handbook of Holographic Interferometry*. Wiley-VCH, 2005.
- [4] U. Schnars and W. P. O. Jüptner, *Digital Holography*. Springer, 2004.
- [5] J. Garcia-Sucerquia, W. Xu, S. K. Jericho, P. Klages, M. H. Jericho, and H. J. Kreuzer, “Digital in-line holographic microscopy,” *Appl. Opt.*, vol. 45, pp. 836–850, 2006.
- [6] K. M. Molony, B. M. Hennelly, D. P. Kelly, and T. J. Naughton, “Reconstruction algorithms applied to in-line gabor digital holographic microscopy,” in preparation.
- [7] G. Pedrini, P. Frning, H. Fessler, and H. J. Tiziani, “Inline digital holographic interferometry,” *Appl. Opt.*, vol. 37, pp. 6262–6269, 1998.
- [8] F. Gori, “Fresnel transform and sampling theorem,” *Opt. Eng.*, vol. 39, pp. 293–297, 1981.
- [9] A. Stern and B. Javidi, “Analysis of practical sampling and reconstruction from fresnel fields,” *Opt. Eng.*, vol. 43, pp. 239–250, 2004.
- [10] Y. Zhang, G. Pedrini, W. Osten, and H. J. Tiziani, “Reconstruction of in-line digital holograms from two intensity measurements,” *Opt. Lett.*, vol. 29, pp. 1287–1289, 2004.
- [11] Y. Frauel, T. J. Naughton, O. Matoba, E. Tajahuerce, and B. Javidi, “Three-dimensional imaging and processing using computational holographic imaging,” *Proc. IEEE*, vol. 94, pp. 636–653, 2006.
- [12] D. Mas, J. Garcia, C. Ferreira, L. M. Bernardo, and F. Marinho, “Fast algorithms for free-space diffraction patterns calculation,” *Opt. Commun.*, vol. 164, pp. 233–245, 1999.
- [13] D. Mas, J. Prez, C. Hernández, C. Vázquez, J. Miret, and C. Illueca, “Fast algorithms for free-space diffraction patterns calculation,” *Opt. Commun.*, vol. 227, pp. 245–258, 2003.
- [14] C. P. McElhinney, J. B. McDonald, A. Castro, Y. Frauel, B. Javidi, and T. J. Naughton, “Depth-independent segmentation of macroscopic three-dimensional objects encoded in single perspectives of digital holograms,” *Optics Letters*, vol. 32, pp. 1229–1231, 2007.
- [15] J. Maycock, C. P. M. Elhinney, B. M. Hennelly, T. J. Naughton, J. B. M. Donald, and B. Javidi, “Reconstruction of partially occluded objects encoded in three-dimensional scenes using digital holograms,” *Applied Optics*, vol. 45, pp. 2975–2985, 2006.
- [16] J. W. Goodman, *Introduction to Fourier Optics*. Roberts & Company Publishers, 2004.
- [17] J. Maycock, B. M. Hennelly, J. B. McDonald, Y. Frauel, A. Castro, B. Javidi, and T. J. Naughton, “Reduction of speckle in digital holography by discrete fourier filtering,” *Journal of Optical Society of America A*, vol. 24, no. 6, pp. 1617–1622, 2007.
- [18] F. H. Y. Chan, F. K. Lam, and H. Zhu, “Adaptive thresholding by variational method,” *IEEE TRANSACTIONS ON IMAGE PROCESSING*, vol. 7, pp. 468–473, 1998.
- [19] G. Bradski and A. Kaehler, *Learning OpenCV Computer Vision with the OpenCV Library*. O'Reilly Media, Inc, 2008.
- [20] S. Suzuki and K. Be, “Topological structural analysis of digitized binary images by border following,” *Computer Vision, Graphics, and Image Processing*, vol. 30, pp. 32–46, 1985.
- [21] K. OConor, H. P. Voorheis, and C. OSullivan, “3d visualisation of confocal fluorescence microscopy data,” *Eurographics Ireland Workshop*, pp. 49–54, 2004.

[22] W. E. Lorensen and H. W. Cline, “Marching cubes  
a high resolution 3d surface construction algorithm,”  
*Computer Graphics*, vol. 21, pp. 163–169, 1987.

[23] U. Tiede, K. H. Hoene, M. Bomans, A. Pommert,  
M. Riemer, and G. Wiebecke, “Investigation of medi-  
cal 3d-rendering algorithms,” *Computer Graphics and  
Applications, IEEE*, vol. 10, pp. 41–52, 1990.